Journal of Hazardous Materials 209–210 (2012) 443–448

Contents lists available at SciVerse ScienceDirect

Journal of Hazardous Materials

journal homepage: www.elsevier.com/locate/jhazmat

TG–MS study of the thermo-oxidative behavior of plastic automobile shredder residues

Qingjie Guo[a,*], Xuan Zhang[a,b], Chao Li[a], Xinmin Liu[a], Jinhui Li[b]

[a] College of Chemical Engineering, Qingdao University of Science and Technology, Qingdao, 266042, PR China
[b] Key Laboratory for Solid Waste Management and Environmental Safety, Chinese Ministry of Education, Tsinghua University, Beijing, 100084, PR China

ARTICLE INFO

Article history:
Received 14 August 2011
Received in revised form
14 December 2011
Accepted 16 January 2012
Available online 23 January 2012

Keywords:
Automobile shredder residues
Thermo-oxidative behavior
TG–MS

ABSTRACT

Automobile shredder residues (ASR) are materials that are rejected in the metal recovery process for end-of-life vehicles (ELV). These residues are composed of such materials as plastics, foams, glasses, rubbers, textiles, remaining metals and soils. ASR disposal is a difficult task, due to increasingly restrictive re-use policies. The pyrolytic reuse of ASR is one important option for energy recovery. The gas release behavior of pyrolyzed ASR was measured using a TG–MS apparatus, and this thermo-oxidative process was observed under different N_2/O_2 volume ratios. The final weight/initial residue weight ratio for pyrolyzed ASR decreased from 43.4% to 10.1% with increasing oxygen concentrations. The production rates of hydrogen, methane and carbon dioxide also varied with different N_2/O_2 volume ratios. The maximum emission of hydrogen and methane occurred when the thermo-oxidative atmosphere was entirely N_2. Temperature had a positive impact on hydrogen production, and the methane emission ratio reached a peak at the second shoulder of the devolatilization stage during which stage organic polymers were emitted. A peculiar characteristic of ASR is its content of nitrogen. The effects of ASR nitrogen content on N_2O and NO_X emissions were investigated in detail. NH_3 was the dominant nitrogen species that was released during ASR pyrolysis. N_2O is highly temperature-sensitive and decomposes to N_2 at temperatures greater than 900 °C.

1. Introduction

The global automotive industry generates approximately 50 million tons of waste each year. Currently, metals account for 75% of the weight of end-of-life vehicles (ELVs) and are almost completely recovered [1]. The remaining 25% is in need of an appropriate waste processing technology other than land-filling. This remaining ELV material that remains after shredding and metal separation is commonly called automobile shredder residue (ASR) or "car fluff". Generally, ASR is a mixture consisting of plastic (19–31%), rubber (20%), textile and fiber materials (10–42%), and wood (2–5%), which are contaminated with metals (8%), oils (5%), and other hazardous components (e.g., polychlorinated biphenyls (PCBs), cadmium, and lead).

ASR composition is highly variable and depends on the generation of vehicles. Since 1990, there has been an increasing demand for the treatment of automobile shredder residue in many countries around the world. Therefore, numerous researchers have begun to focus significant attention on ASR disposal.

To date, the dominant disposal route for ASR has been landfilling, which may pollute soils and groundwater resources. Therefore, the development of technology that can recover usable materials and minimize ASR volume has become an important issue [2]. Thermal treatment (e.g., pyrolysis and gasification) is an ideal approach for transforming ASR into environmentally harmless and lower-volume substances while simultaneously recovering energy, which is a more sustainable and effective waste management practice.

Pyrolysis is considered to be a chemical recycling process, due to the breaking of long polymeric chains into smaller molecules of the same chemical structure. However, the presence of chlorine and bromine in materials undergoing pyrolysis is undesirable. The elimination of these elements is a major consideration in developing processes for mixed plastics disposal as residual chlorine and bromine distribute over the resulting products. As expected, the pyrolysis process is an attractive option because it reduces corrosion and emissions of sulfur, chlorine, and Polychlorinated Dioxins and Furans (PCDD/F) without sacrificing the alkali metals (except mercury and cadmium). Meanwhile, pyrolysis lowers the rate of thermal NO_X formation, due to its lower reaction temperatures. The technical challenge is to increase H_2 production efficiency from the thermo-oxidative process of ASR processing. The gas produced by these processes can be used in many applications,

* Corresponding author. Tel.: +86 532 84022506; fax: +86 532 84022757.
E-mail address: qj_guo@yahoo.com (Q. Guo).

0304-3894/$ – see front matter © 2012 Elsevier B.V. All rights reserved.
doi:10.1016/j.jhazmat.2012.01.051

Table 1
Elements analysis of automobile shredded residues.

Elemental analysis (%)				Proximate analysis (%)				
C	H	N	S	Moisture	Ash	Volatiles	Fixed carbon	HHV (MJ/kg)
48.82	5.63	0.95	0.50	2.06	12.33	52.71	32.9	24.5

such as in chemical synthesis (e.g., raw material syngas) and in Fisher–Tropcsh fuel syntheses.

Thermogravimetric (TG) analysis is one of the most commonly used techniques to explore the primary reactions of the decomposition of solids [3,4]. To investigate the thermal degradation of wastes, various TG techniques have been used; for instance, TG was used in the study of the degradation of tires by Díez et al. [5], and TG–DSC was employed by Pacewska et al. [6] and Heikinen and Spliethoff [7]. Generally, TG illustrates the thermal decomposition in terms of the mass loss, whereas TG–MS extends the thermal analysis by the additional monitoring and identification of the gasification gases. It is obvious that the study of decomposition profits greatly from this additional information, which provides detailed insight into the decomposition processes. The use of TG in combination with MS is more suitable for identifying the materials produced, as is the case in many other applications [6,7], than is the use of TG with a mass-selective detector [8,9].

Many authors [10–16] have published papers on gas emissions from the combustion or co-combustion of different materials, such as medical waste [10], biomass [11], and poultry litter [12], and others have examined the emissions from gasification [16] and pyrolysis reactions [5,17]. For our TG–MS apparatus, the released compounds were analyzed in situ during the entire thermo-oxidative process, and the apparatus was only constrained by detecting and identifying the most abundant species. No studies have been published regarding gas emissions from four thermo-oxidative degradation processes of ASR.

This paper analyses gas emissions from the processes of heating ASR under different oxygen concentrations using TG–MS analysis. The online evolution of the major volatile degradation products was monitored over the course of each reaction. A comparison between the evolved gas phases measured using TG–MS during the combustion of ASR under the different atmospheres studied is presented subsequently. The objective of this test was to study the thermo-oxidative ASR conversion processes themselves and to compare the gas emissions from each of these processes.

2. Experiments

2.1. ASR samples

The representative ASR samples used in this study included polypropylene (PP) bumper material, polyurethane (PU) car roofing material, and gasket material; these materials were pulverized to a mesh size smaller than 0.1 mm. The elemental analysis and proximate analysis of the ASR used are listed in Table 1. Further, the high heating value (HHV) at a constant volume was measured with a well-8000 adiabatic oxygen bomb calorimeter (Mingrui Instrument Co. Ltd., Shanhai, China).

2.2. Experimental instruments

The thermo-oxidative processes of all of the samples were measured using a METTLER TOLEDO TGA/DSC1 STAR^e thermogravimetric analyzer, the exit of which was connected to the capillary of an OmniStar^{TM} mass spectrometer. This coupling allows the relative concentrations of the gases emitted to be determined at near-equilibrium conditions. Meanwhile, the length of the gases emitted during the thermal conversion process was monitored by the MS. The thermo-oxidative processes of all of the samples were performed using a thermogravimetric analyzer. To simulate gasification and pyrolysis, four atmospheres with different molar ratios of nitrogen to oxygen, specifically, 100%, 95%, 90%, and 80% nitrogen, were examined at the same flow rate of 100 mL min^{-1}. A value of 100% nitrogen is representative of a pyrolysis process, and the other values represent gasification processes. Each sample was analyzed under gradient heating conditions with a heating rate of 30 K min^{-1} from 30 °C to 1000 °C.

A silica capillary column was kept in the thermo gravimetric analyzer to feed emission gases into the connected mass spectrometer. The gases released from the solid sample into the thermogravimetric analyzer were directly fed into the ionization chamber of the mass spectrometer. The TG–MS interface gives the plot of a selected m/z as a function of ion current (IC), which can monitor the evolution of a single specific molecular species (during the entire thermal process), if this ion arises solely from the fragmentation pattern of that chemical species.

The ion currents for different fragments are plotted with the corresponding TG data. In theory, distinct decomposition pathways result in the formation of different characteristic ions. Key ions or typical series of fragments indicate the release of a given gaseous species during the thermo-oxidative process. Accordingly, the distinct molecular origins of the different processes can often be determined.

During the thermo-oxidative degradation of ASR, TG–MS was employed to identify the gaseous emissions corresponding to the observed m/z values, as shown in Table 2. Emissions with m/z = 44, 46, and 64 were mainly attributable to CO_2, NO_2 and SO_2 as the most probable parent molecules [1], which are especially problematic species from an environmental viewpoint. A detailed identification of the gaseous species evolved during the thermal treatment up to 1000 °C is also presented. Nitrogen was used for the inert atmosphere because N_2 has the same molecular mass as CO, which makes CO difficult to determine by mass spectrometry. No appreciable changes were detected in the TG profiles.

3. Results and discussion

3.1. Thermo-oxidative process

As shown in Fig. 1, nitrogen was the representative gas of the pyrolysis process. The final weight-loss ratio increased with increasing concentrations of oxygen, indicating that the higher oxygen concentration in the reaction gas resulted in the reaction's proceeding to completion. As the oxygen concentration increased, the final weight-residual ratio of the ASR decreased from 43.4%

Table 2
Relationships between mass number (m/z), fragment and probable parent molecule.

m/z	Key fragment	Probable parent molecule
2	H_2^+	H_2
15	CH_3^+	CH_4
30	$C_2H_6^+$, NO^+	C_2H_6, NO
44	CO_2^+, N_2O^+	CO_2, N_2O
46	NO_2^+	NO_2
64	SO_2^+	SO_2

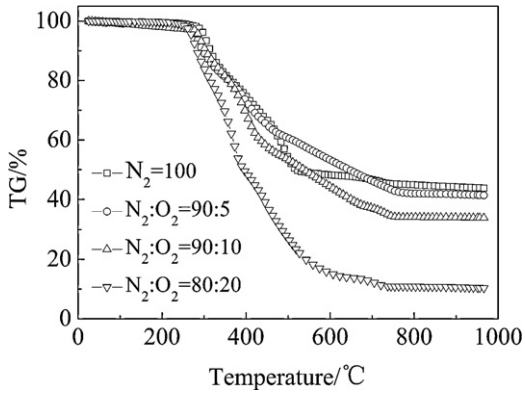

Fig. 1. TG curves of ASR degradation under different atmospheres at a heating rate of 30 K min^{-1}.

to 10.1%. The weight-residual ratio of the ASR was 43.4% nitrogen (mass percent) with a volatile composition of 56.6% (mass percent), which approximates the volatile composition percentage of ASR obtained using proximate analysis (52.71%).

There was only slight weight loss at temperatures lower than 200 °C, which was attributed to water volatilization from the ASR. However, the weight of the ASR decreased rapidly at temperatures ranging from 250 °C to 550 °C. A considerable quantity of volatile components was emitted in this stage, suggesting that polymers in the ASR were decomposed into volatile components with smaller molecular weights. Note that the thermo-oxidative emission processes of each component clearly changed because the compositions of the ASR samples exhibited complications at this stage. As shown in Fig. 1, the curve of TG under the nitrogen atmosphere revealed that the volatile compounds were separated with asphaltum oil and gas released over the 250–550 °C range. At temperatures exceeding 500 °C, no obvious weight-loss peaks were observed because a second gas emission stage occurred. The carbon generated during the decomposition process of the ASR reacted with oxygen, yielding such gases as CO, CO_2, H_2, and CH_4. Finally, the thermo-oxidative process was complete as the temperature approached 720 °C.

3.2. Gas emissions

A mass spectrometry analysis was employed to evaluate gas species based on their molecular masses corresponding to mass number (m/z) signals. A series of experiments are depicted in Figs. 2–10. The gas species, which evolved throughout the thermal chemical processing of ASR samples at temperatures of up

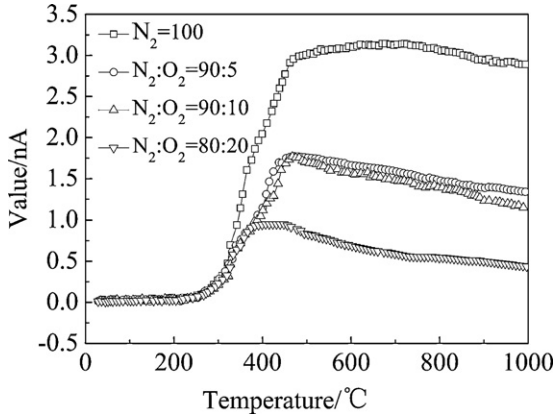

Fig. 2. H_2 emission as a function of temperature under different atmospheres.

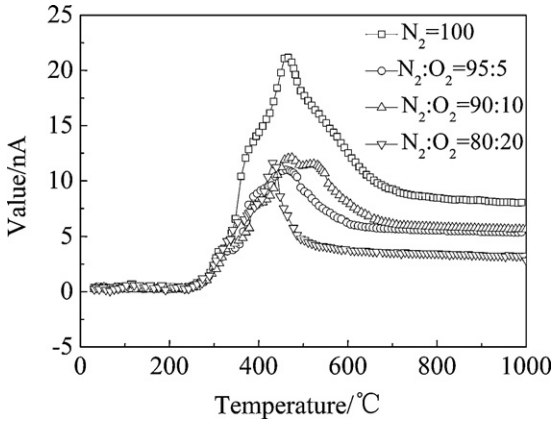

Fig. 3. CH_4 emission as a function of temperature under different atmospheres.

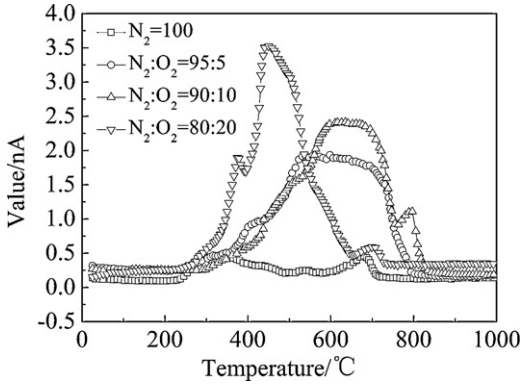

Fig. 4. NO_2 emission as a function of temperature under different atmospheres.

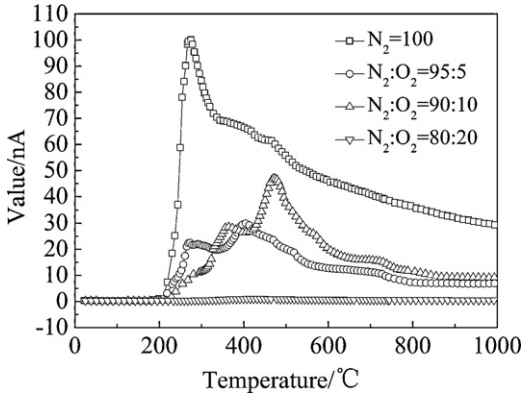

Fig. 5. NH_3 emission as a function of temperature under different atmospheres.

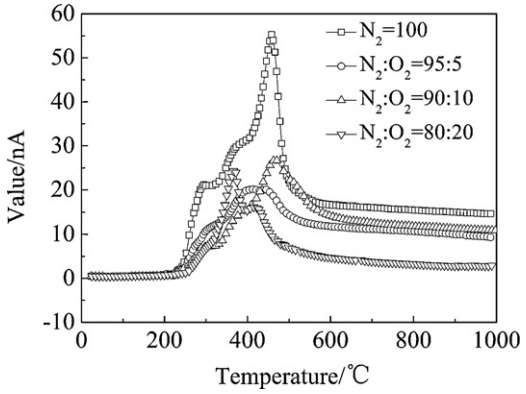

Fig. 6. HCN emission as a function of temperature under different atmospheres.

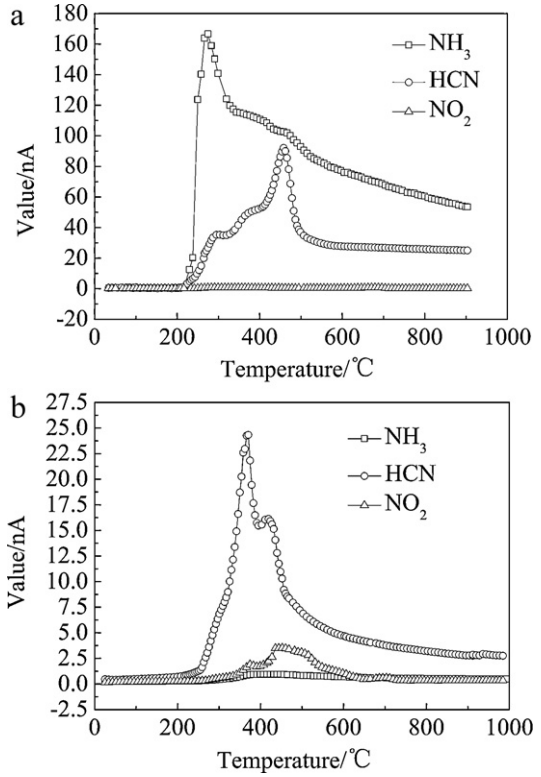

Fig. 7. Emission characteristics of NH3, HCN and NO2 as functions of temperature under different atmospheres (a: N_2 = 100; b: N_2:O_2 = 80:20).

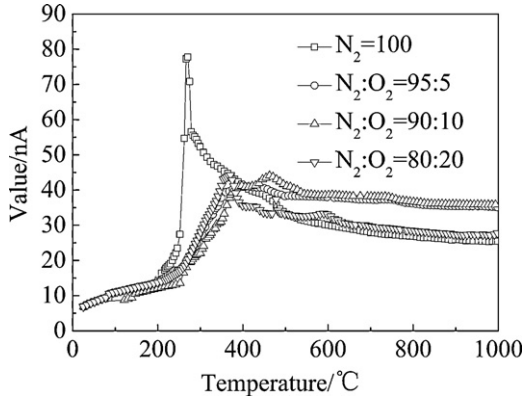

Fig. 8. C_2H_6 and NO emissions as functions of temperature under different atmospheres.

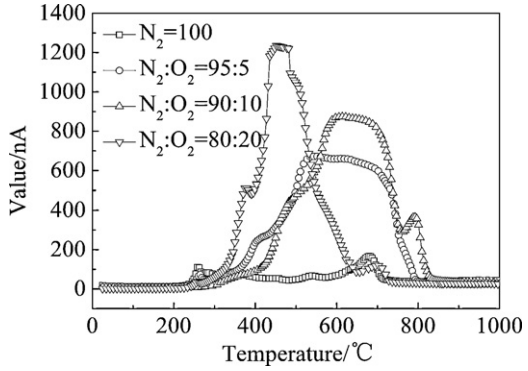

Fig. 9. CO_2 and N_2O emissions as functions of temperature under different atmospheres.

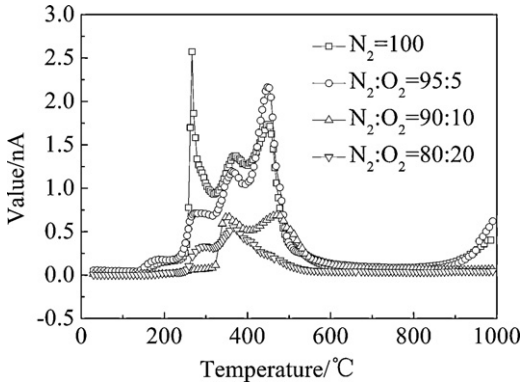

Fig. 10. SO_2 emissions as a function of temperature under different atmospheres.

to 1000 °C, can be analyzed by the appropriate m/z signal. Previous studies have shown that thermal reaction processes depend on the atmosphere, including nitrogen and mixtures of nitrogen with oxygen. The gas evolutions are discussed in the following sections.

3.2.1. Permanent gas evolution

To explore the emission of gases produced by the degradation of the ASR samples, the following reactions between gases, steam, and carbon (char) should be considered [18]:

$$\text{Oxidation } C(s) + O_2 \leftrightarrow CO_2 \quad Q = 407.4\,\text{kJ/mol} \tag{1}$$

$$\text{Partialoxidation } C(s) + 1/2O_2 \leftrightarrow CO \quad Q = 126.4\,\text{kJ/mol} \tag{2}$$

$$\text{Boudouardreaction } C(s) + CO_2 \leftrightarrow 2CO \quad Q = -173.8\,\text{kJ/mol} \tag{3}$$

$$\text{Steamcarbonreaction } C(s) + H_2O \leftrightarrow CO + H_2 \quad Q = -131\,\text{kJ/mol} \tag{4}$$

$$\text{Watergasshiftreaction } CO + H_2O \leftrightarrow CO_2 + H_2 \quad Q = 43.47\,\text{kJ/mol} \tag{5}$$

$$\text{Methanesteamreforming } CH_4 + H_2O \leftrightarrow CO + 3H_2 \quad Q = -206.4\,\text{kJ/mol} \tag{6}$$

$$\text{Methanedryreforming } CH_4 + CO_2 \leftrightarrow 2CO + 2H_2 \quad Q = -247.3\,\text{kJ/mol} \tag{7}$$

$$\text{Methanation } C(s) + 2H_2 \leftrightarrow CH_4 \quad Q = 74.82\,\text{kJ/mol} \tag{8}$$

The value of m/z = 2 corresponds to the emission of hydrogen, which is regarded as a clean energy source with a high caloric value of 41.22 MJ Nm^{-3}. The maximum emission level of hydrogen for ASR occurs when nitrogen is employed in the heating atmosphere. Fig. 2 shows that increased temperatures favor hydrogen production, possibly because hydrogen production has a preference for Reactions (4)–(7). As the reactions proceeded, the hydrogen concentrations in the effluent gas decreased slightly, due to the occurrence of methanation in Reaction (8). In particular, Fig. 2 indicates that the rate of hydrogen generation increased significantly at 470 °C when the C—C and C—H bond breaking reactions become thermally activated.

Hydrocarbons were released primarily over a temperature range of 260–620 °C, which can be directly observed by following the trend of the m/z = 15 ion current in Fig. 3. Methane is produced in the fragmentation process of every methyl-containing organic compound. For the pyrolysis process, an intense peak occurs at

475 °C under a nitrogen atmosphere. We found that the highest methane emission level appeared under an inert atmosphere (100% nitrogen), which corresponded to the simulated pyrolysis process. Methane emission levels decreased as oxygen content increased. Such differences can be observed under different heating conditions that simulate the thermo-oxidative process. Note that methane emissions peaked at the second shoulder of the devolatilization stage, during which stage organic polymers were further decomposed.

3.2.2. Pollutant gas evolution

There is a growing interest in the removal of organic carbon and acidic gases, such as SO_2 and NO_X, from flue gases. It is well known that such gases can cause severe acid-rain events, ozone destruction, and global warming [3]. The emission characteristics of these components from ASR thermo-oxidative degradation reactions depend largely upon the S and N content of the ASR to be processed. Generally, most of the sulfur in ASR is released as SO_2 during thermo-oxidative processing. Malkow [19] reported that the gasification processes can handle plastic waste mixtures and that high carbon conversion is achieved at high temperatures with low tar production.

Nitrogen dioxide generation corresponds to a TG–MS peak at $m/z = 46$. Numerous investigations have demonstrated that NO_X is the dominant component of photochemical fog and acid rain. As indicated in Fig. 4, no NO_2 is produced during pyrolysis under a 100% nitrogen atmosphere (without oxygen). NO_2 concentrations increased with increasing oxygen fractions in a mixture of N_2 and O_2. This result means that an increased availability of oxygen promoted the release of fuel nitrogen from the solid into the gas phase with respect to other dry components. The same conclusions were obtained by Chen et al. [20] using coal pellets. Under an oxygen atmosphere, in Figs. 4–6, NH_3 and HCN reached their maximum levels during coal pellet combustion, whereas NO_2 concentration increased as the temperature increased to 480 °C. It has been experimentally shown that the most fuel NO_X that is released during devolatilization is converted to HCN, which is consistent with the findings of Ponzio et al. [21]. Furthermore, the release of NO_2 decreases with increasing oxygen concentrations. However, the emissions of NH_3 and HCN decrease with increasing oxygen concentrations. As illustrated in Fig. 7, the total amount of NO_X emitted during the thermo-oxidative process can be calculated by summing the emissions of HCN and NH_3 from the ASR gasification process. Small volatile molecules are released first, and fuel-nitrogen subsequently decomposes to NO_X and N_2 via a series of radical reactions. Nitrogen dioxide was released through the ignition stage under thermo-oxidative heating atmospheres.

The formation mechanism of NO_X from fuel nitrogen is more complex. During the devolatilization of ASR, a portion of fuel nitrogen is released with the volatiles, and the remaining part is retained in the char. NO_X is generated by two routes; one is through the gas phase oxidation of nitrogenous groups in the volatiles, and the other is through the heterogeneous oxidation of char-bound nitrogen species. In the former case, NH_3 can decompose into NH_2 and NH radicals, which can either be oxidized by oxygen to produce NO or react with available NO and OH radicals to yield N_2. Accordingly, NH_3 is both a source and a reducing agent of NO radicals, depending upon the prevailing circumstances. The other volatile nitrogenous component, HCN, can decompose to NCO with the help of an oxygen radical; therefore, NCO can react with NO to form N_2O [22]. With respect to the char-bound nitrogen, single particle combustion experiments showed that the main nitrogen species formed during the combustion of char are N_2O and N_2, with NO concentrations being higher than N_2O concentrations and with NO and N_2O formation being proportional to the degree of carbon burn-out [23]. N_2O formation is highly temperature-sensitive, as this species decomposes to N_2 and O_2 at temperatures higher than 900 °C. In summary, NH_3 is the dominant nitrogen species released during ASR pyrolysis.

As illustrated in Fig. 8, ethane and nitrogen monoxide are both identified at an m/z value of 30. No emissions are also detected at $m/z = 46$, and the shoulder of the curves correspond to ethane. For the $m/z = 30$ and $m/z = 46$ curves, it can be concluded that NO emissions might be associated with the ignition-and-burning stage, although N_2O emissions occurred at the final volatilization phase when the atmosphere is totally reactive. At the devolatilization stage, NO_2 could be observed, and ethane was released. No ignition occurred under a nitrogen atmosphere; accordingly, the $m/z = 30$ curve must have only been associated with ethane, and these emissions attained their maximum value under these conditions.

Fig. 9 indicates that CO_2 and N_2O emissions were associated with $m/z = 44$, and, as described, the MS ion curves of carbon dioxide correspond to an m/z value of 44 for all the samples studied, as shown in Table 2. N_2O was released during the ignition-and-burning stage. As mentioned previously, CO_2 emissions were observed under all heating atmospheres for ASR, but lower emissions occurred under gasification atmospheres (N_2 95, N_2 90 and N_2 80). Clearly, the CO_2 evolution trend presents two overlapping peaks at 240 and 320 °C followed by a shoulder at 430 °C and by less intense peaks at 610 and 700 °C. Nevertheless, this signal is also present in the mass spectrum of CO_2 and even in the fragmentation pattern of other species, which are released in lower amounts. This ion current presents two overlapping bands at 240 and 325 °C followed by a broad peak at 470 °C (corresponding with the evolution of the hydrocarbon mixture) and by two more intense peaks at 710 and 760 °C.

SO_2 emissions in a pulverized flame were strongly dependent on the sulfur content of the ASR. For combustion, 90–100% of the sulfur in the ASR was converted into SO_2, with a higher fuel S input, resulting in linearly higher SO_2 emissions.

SO_2 was emitted at an m/z value of 64, as shown in Fig. 10. Emissions of SO_2 were detected under all heating atmospheres. The peak of SO_2 concentrations appeared under $N_2/O_2 = 80/20$ because the higher oxygen concentration produced greater SO_2 yields. SO_2 was formed under the 100% nitrogen atmosphere, due to the presence of oxygen in the ASR composition. One can thus observe that SO_2 emissions increase with increasing oxygen concentrations.

4. Conclusions

From the previous investigation, we can make the following conclusions.

(1) As the oxygen content increases, the final weight-residual ratio of the processed ASR declines from 43.4% to 10.1%.
(2) The maximum emission of hydrogen for ASR occurred when the heating atmosphere was entirely nitrogen. Less hydrogen was emitted under gasification atmospheres containing oxygen. An increase in temperature resulted in increased hydrogen production.
(3) The maximum methane emissions for ASR processing were observed under a totally inert (100% nitrogen) atmosphere. Methane emissions decreased as atmospheric oxygen content increased. For ASR, the greatest methane emissions occurred at the second shoulder of the devolatilization stage because organic polymers were emitted during that stage.
(4) A peculiar characteristic of ASR is its content of nitrogen. NH_3 is the dominant nitrogen species released during the thermo-oxidative treatment of ASR.

In summary, the thermo-oxidative treatment of ASR by gasification appears to be an attractive alternative for sustainable waste management. Furthermore, apart from the energy recovery and environmental discharge considerations, the absence of landfilling costs is another factor that promotes the use of thermo-oxidative treatment.

Acknowledgment

Financial support from the National Sciences Foundation of China (no. 20876079), the Key Laboratory for Solid Waste Management and Environment Safety, the Ministry of Education of China (no. swmes 2009-05) and theScience Foundation for Distinguished Young Scholars of Shandong Province (JQ200904) is greatly appreciated.

References

[1] F. Viganò, S. Consonni, M. Grosso, L. Rigamonti, Material and energy recovery from Automotive Shredded Residues (ASR) via sequential gasification and combustion, Waste Manag. 30 (2010) 145–153.
[2] H. Mitsuo, I. Shuji, Development of Automobile Shredder residue (ASR) dry distillation/gasification technology, Trans. Soc. Automot. Eng. Jpn. 32 (2001) 139–144.
[3] J.A. Reyes, J.A. Conesa, A. Marcilla, Pyrolysis and combustion of polycoated cartons: kinetic model and MS-analysis, J. Anal. Appl. Pyrolysis 59 (2001) 747–763.
[4] M.J. Cuesta, F. Rubiera, A. Arenillas, M.J. Iglesias, I. Suarez-Ruiz, et al., Evaluation of the combustion behaviour of perhydrous coals by thermal analysis, J. Therm. Anal. Calorim. 81 (2005) 333–337.
[5] C. Díez, O. Martínez, L.F. Calvo, et al., Pyrolysis of tyres: influence of the final temperature of the process on emissions and the calorific value of the products recovered, Waste Manag. 24 (2004) 463–469.
[6] B. Pacewska, A. Klepariska, P. Stefaniak, D. Szychowski, J. Therm. Anal. Calorim. 60 (2000) 229–236.
[7] J. Heikinen, H. Spliethoff, Waste mixture composition by thermogravimetric analysis, J. Therm. Anal. Calorim. 72 (2003) 1031–1039.
[8] E. Meszaros, E. Jakab, G. Varhegyi, P. Tovari, Thermogravimetry/mass spectrometry analysis of energy crops, J. Therm. Anal. Calorim. 88 (2007) 477–482.
[9] M. Ischia, C. Perazzolli, R. Dal Maschio, R. Campostrini, Pyrolysis study of sewage sludge by TG–MS and TG–GC–MS coupled analyses, J. Therm. Anal. Calorim. 87 (2007) 567–574.
[10] T. Arii, A. Kishi, Humidity controlled thermal analysis: the effect of humidity on thermal decomposition of zinc acetylacetonate monohydrate, J. Therm. Anal. Calorim. 83 (2006) 253–260.
[11] A. Pappa, K. Mikedi, N. Tzamtzis, M. Statheropoulos, TG–MS analysis for studying the effects of fire retardants on the pyrolysis of pine-needles and their components, J. Therm. Anal. Calorim. 84 (2006) 655–661.
[12] A. Onishi, P.S. Thomas, B.H. Stuart, J.P. Guerbois, S. Forbes, TG–MS analysis of the thermal decomposition of pig bone for forensic applications, J. Therm. Anal. Calorim. 88 (2007) 405–409.
[13] M.C.M. Alvim-Ferraz, S.A.V. Afonso, Incineration of different types of medical wastes: emission factors for gaseous emissions, Atmos. Environ. 37 (2003) 5415–5422.
[14] V.I. Kouprianov, W. Permchart, Emissions from a conical FBC fired with a biomass fuel, Appl. Energy 74 (2003) 383–392.
[15] A.M. Henihan, M.J. Leahy, J.J. Leahy, E. Cummins, B.P. Kelleher, Emissions modeling of fluidised bed co-combustion of poultry litter and peat, Bioresour. Technol. 87 (2003) 289–294.
[16] H. Liu, B.M. Gibbs, Modeling NH_3 and HCN emissions from biomass circulating fluidized bed gasifiers, Fuel 82 (2003) 1591–1604.
[17] L. Zhang, A. Sato, Y. Ninomiya, E. Sasaoka, Partitioning of sulfur and calcium during pyrolysis and combustion of high sulfur coals impregnated with calcium acetate as the desulfurization sorbent, Fuel 83 (2004) 1039–1053.
[18] R. Ray, R.B. Thorpe, A comparison of gasification with pyrolysis for the recycling of plastic containing wastes, Int. J. Chem. React. Eng. 5 (2007) A85.
[19] T. Malkow, Novel and innovative pyrolysis and gasification technologies for energy efficient and environmentally sound MSW disposal, Waste Manag. 24 (2004) 53–79.
[20] J.C. Chen, C. Castagnoli, S. Niksa, Coal devolatilization during rapid transient heating. 2. Secondary pyrolysis, Energy Fuel 6 (1992) 264–271.
[21] A. Ponzio, S. Senthoorselvan, W. Yang, W. Blasiak, O. Eriksson, Nitrogen release during thermochemical conversion of single coal pellets in highly preheated mixtures of oxygen and nitrogen, Fuel 88 (2009) 1127–1134.
[22] J.A. Miller, C.T. Bowman, Mechanism and model of nitrogen chemistry in combustion, Prog. Energy Combust. Sci. 15 (1989) 287–338.
[23] M.R. Klein, G. Rotzoll, N_2O and NO_x formation during coal and char combustion in a fluidized bed, VGB Kraftwerktechnik 74 (1994) 1072–1080.